

Terrestrial Gamma-ray Flashes Can Be Detected with Radio Measurements of Energetic In-cloud Pulses during Thunderstorms

Fanchao Lyu¹, Steven A. Cummer², Michael S. Briggs³, David M. Smith⁴, Bagrat Mailyan⁵, and Stephen Lesage³

¹Nanjing Joint Institute for Atmospheric Sciences

²Duke University

³University of Alabama in Huntsville

⁴University of California, Santa Cruz

⁵New York University Abu Dhabi

November 23, 2022

Abstract

Many of the details of how terrestrial gamma-ray flashes (TGFs) are produced, including their association with upward-propagating in-cloud lightning leader channels, remain poorly understood. Measurements of the low-frequency radio emissions associated with TGF production continuously provide unique views and key insights into the electrodynamics of this process. Here we report further details on the connection between energetic in-cloud pulses (EIPs) and TGFs. With coordinated measurements from both the ground-based radio sensors and space-based gamma-ray detectors on the Fermi and RHESSI spacecraft, we find that all ten +EIPs that occurred within the searched space-and-time window are associated with simultaneous TGFs, including two new TGFs that were not previously identified by the gamma-ray measurements alone. The results in this study not only solidify the tight connection between +EIPs and TGFs, but also demonstrate the practicability of detecting a subpopulation of TGFs with ground-based radio sensors alone.

1 **Terrestrial Gamma-ray Flashes Can Be Detected with Radio Measurements of**
2 **Energetic In-cloud Pulses during Thunderstorms**

3

4 Fanchao Lyu^{1,2}, Steven A. Cummer^{3*}, Michael Briggs⁴, David M. Smith⁵, Bagrat
5 Mailyan⁶, Stephen Lesage⁴

6

7 ¹Nanjing Joint Institute for Atmospheric Sciences, Nanjing, Jiangsu, China

8 ²State Key Laboratory of Severe Weather, Chinese Academy of Meteorological
9 Sciences, Beijing, China

10 ³Electrical and Computer Engineering Department, Duke University, Durham, North
11 Carolina, USA

12 ⁴CSPAR, University of Alabama in Huntsville, Huntsville, Alabama, USA

13 ⁵Physics Department, University of California Santa Cruz, Santa Cruz, California,
14 United States

15 ⁶Center for Astro, Particle and Planetary Physics, New York University Abu Dhabi,
16 Saadiyat Marina District, Abu Dhabi, UAE

17

18 * Correspondence to: cummer@ee.duke.edu

19

20

21

22

23 **Key point:**

- 24 • Positive polarity energetic in-cloud pulses produce TGFs with high-to-certain
25 probability (74% - 100%)
- 26 • New TGFs previously missed by space-based detectors were found by ground
27 detection of +EIPs
- 28 • Demonstrated that a subset of TGFs can be found from remote ground-based
29 radio detection alone

30

31 **Abstract**

32 Many of the details of how terrestrial gamma-ray flashes (TGFs) are produced,
33 including their association with upward-propagating in-cloud lightning leader channels,
34 remain poorly understood. Measurements of the low-frequency radio emissions
35 associated with TGF production continuously provide unique views and key insights
36 into the electrodynamics of this process. Here we report further details on the
37 connection between energetic in-cloud pulses (EIPs) and TGFs. With coordinated
38 measurements from both the ground-based radio sensors and space-based gamma-ray
39 detectors on the Fermi and RHESSI spacecraft, we find that all ten +EIPs that occurred
40 within the searched space-and-time window are associated with simultaneous TGFs,
41 including two new TGFs that were not previously identified by the gamma-ray
42 measurements alone. The results in this study not only solidify the tight connection
43 between +EIPs and TGFs, but also demonstrate the practicability of detecting a
44 subpopulation of TGFs with ground-based radio sensors alone.

45

46 **1. Introduction**

47 Terrestrial gamma-ray flashes (TGFs) are a kind of high energy emissions (up
48 to several tens of MeV) that are generated during thunderstorms and are generally
49 detected by space-based gamma-ray photon detectors (*Fishman et al., 1994; Smith et*
50 *al., 2005; Briggs et al., 2010; Marisaldi et al., 2010; Neubert et al., 2020*). Ground-
51 based radio measurements and modeling of the discharge processes associated with
52 TGFs suggest that low frequency (LF) radio emissions are usually generated during
53 TGF production (*Connaughton et al., 2010; Cummer et al., 2011; Lu et al., 2011;*
54 *Dwyer et al., 2012; Dwyer & Cummer, 2013; Cummer et al., 2014; Dwyer et al., 2017;*
55 *Lyu et al., 2018; Roberts et al., 2018; Pu et al., 2019; Zhang et al., 2020*), but the details
56 of these LF signals still need further investigation.

57 More specifically, a recent study reported a distinct lightning process called
58 energetic in-cloud pulses (EIPs) that occur during the propagation of some negative
59 leaders and produce high equivalent peak current pulses (*Lyu et al., 2015; Lyu &*
60 *Cummer, 2018*). The similarity of the radio emissions between that associated with a
61 subset of TGFs (*Lu et al., 2011; Cummer et al., 2014*) and that of EIPs raised the
62 question of whether EIPs and TGFs two faces of the same phenomenon. Lyu et al. (*Lyu*
63 *et al., 2016*) addressed that question using 3 EIPs that were identified from radio
64 measurements alone that occurred within the gamma-ray detection range (500 km
65 horizontally) of the Fermi Gamma-ray Burst Monitor (GBM) instrument (*Briggs et al.,*
66 *2010*). The known location and time of these 3 EIPs enabled a search for associated
67 TGF gamma-rays in a narrow 100-microsecond time window. Interestingly, all three
68 events contained significant gamma-ray flux simultaneous with the EIPs, showing that
69 the three EIPs were all also TGFs (*Lyu et al., 2016*). In addition, the similar occurrence
70 contexts (*Stanley et al., 2006; Lu et al., 2010; Shao et al., 2010; Cummer et al., 2011;*

71 *Østgaard et al.*, 2013; *Lyu et al.*, 2018; *Pu et al.*, 2019) and event occurrence frequency
72 between EIPs and TGFs within the Fermi-observed area further support the idea that at
73 least a significant fraction of EIPs are also TGFs (*Lyu et al.*, 2016). A recent study
74 from the observations with the Atmosphere Space Interactions Monitor (ASIM)
75 (*Neubert et al.*, 2019), onboard the International Space Station (ISS), showed a
76 terrestrial gamma-ray flash (TGF) associated with elves produced during the initial
77 leader of a lightning flash (*Neubert et al.*, 2020). The associated radio signal was likely
78 an EIP of positive polarity, which also confirmed the model study on the possible
79 relationship between TGFs and Elves through a common association with EIPs (*Liu et*
80 *al.*, 2017).

81 These studies suggested a strong connection between EIPs, TGFs, and other
82 phenomena. Even though only a subset (~10%) of TGFs are associated with the
83 extremely high equivalent peak current radio emissions of EIPs (*Lu et al.*, 2011;
84 *Cummer et al.*, 2014), this finding on the EIP-TGF relationship opens the possibility
85 that a portion of the overall TGF population could be identified from ground-based
86 radio measurements alone. The 3 out of 3 EIP-TGF pairs and their similar occurrence
87 contexts enabled the hypothesis that every +EIP is also a TGF (*Lyu et al.*, 2016). This
88 study aims for improved statistics to answer the two fundamental questions: Are all
89 EIPs identified from radio emissions alone also TGFs? And is it possible to detect a
90 subset of TGFs by searching the ground measurements of EIPs alone?

91 We report here the analysis of an enlarged, 5-year database of EIPs that occurred
92 during Fermi and RHESSI satellite overpasses. We find that a total of 10 out of 10
93 +EIPs are associated with detected TGFs that are essentially simultaneous with the EIPs.
94 This includes the 3 +EIPs previously reported by *Lyu et al.* (*Lyu et al.*, 2016), 5 new
95 EIPs associated with previously identified TGFs, and importantly 2 new EIP-TGFs that

96 were not previously identified from gamma-ray measurements alone. One of these was
97 detected by the Fermi Gamma-ray Burst Monitor (GBM) (*Briggs et al.*, 2010), and one
98 was detected by the Reuven Ramaty High Energy Solar Spectroscopic Imager (RHESSI)
99 (*Smith et al.*, 2005). That 10 out of 10 independently identified +EIPs are also found
100 to be simultaneous TGFs implies a high-to certain probability of 74%-100% that any
101 given +EIP is also TGF. It is especially noteworthy that a search for +EIPs from the
102 ground radio measurements alone identified two previously unreported TGFs from two
103 different space-based platforms. This not only provides strong evidence of the
104 connection between +EIPs and TGFs, but also demonstrates the practicability of
105 detecting a subpopulation of TGFs from ground-based radio measurements alone.

106

107 **2. Instrumentation**

108 The analysis in this study was conducted with a comprehensive investigation of
109 radio signals of +EIPs and the gamma-ray photons in a short time window of several
110 hundred microseconds around the time of the +EIPs. +EIPs were identified from a
111 combination of high peak current NLDN events and the corresponding radio emissions,
112 which includes the low frequency (LF), very low frequency (VLF), and ultra-low
113 frequency (ULF) radio sensors operated by Duke University (*Lyu et al.*, 2015; *Lyu et*
114 *al.*, 2016). The +EIPs were identified with the same approach used by *Lyu et al.* (2016)
115 by accumulating NLDN-reported lightning events above a peak current threshold (150
116 kA or 200 kA, depending on the year) and within a given maximum range (1000 or
117 2000 km, again depending on the year) from one of our LF radio sensors deployed
118 around the United States. All the NLDN-reported positive ICs, positive CGs, and
119 negative ICs that exceeded the peak current threshold were selected for waveform

120 analysis. We then used VLF and LF radio waveforms to classify each of these lightning
121 events as CG, NBE, or EIP based on the automated process described previously (*Lyu*
122 *et al.*, 2015). The positive EIPs were sorted out based on their radio signal polarity.

123 The +EIPs identified during two periods were analyzed in this study: either from
124 a four-year database between 2014 and 2017, or from the year 2012. The two periods
125 of +EIPs were selected corresponding to the two different space-based gamma-ray
126 detection platforms, respectively, which are the Fermi-GBM (*Briggs et al.*, 2010) and
127 the RHESSI gamma-ray detector (*Smith et al.*, 2005). This population of +EIPs is then
128 analyzed based on the horizontal distance from the Fermi or RHESSI satellite footprint
129 at the time, and for those events sufficiently close, we examine the gamma-ray counts
130 from each instrument at the precise time predicted by the known +EIP location and time.

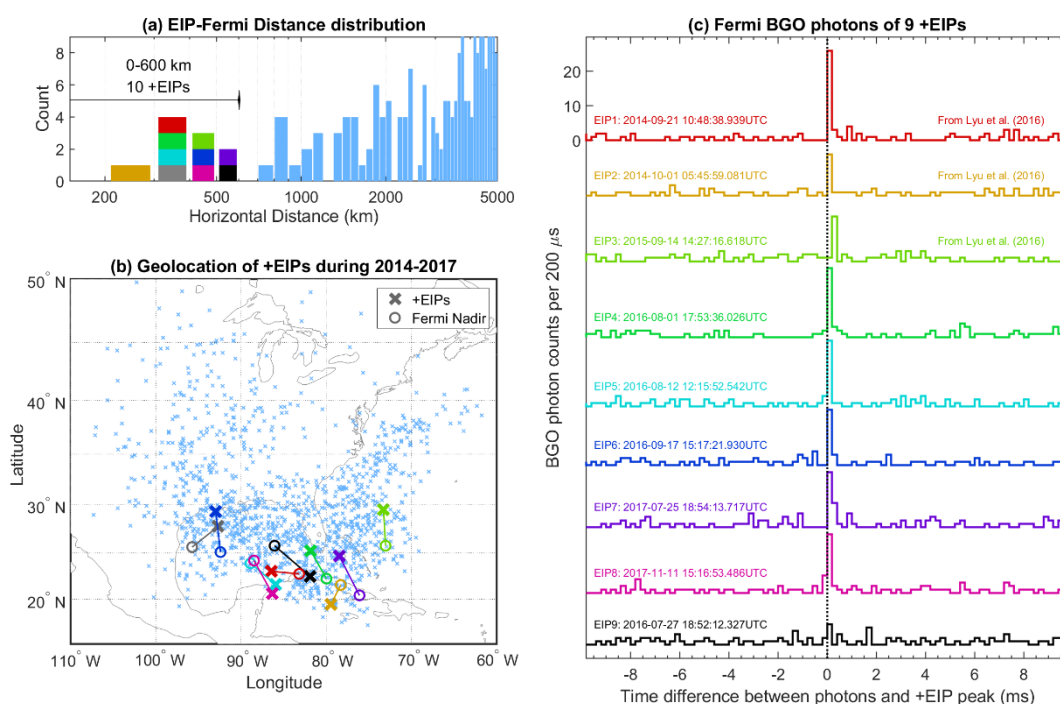
131

132 **3. +EIPs identified during a four-year survey and the TGF signature of +EIPs** 133 **recognized by Fermi-GBM**

134 From the radio measurement database during 2014–2017, a total of 1334 events
135 were identified by the radio signals to be +EIPs. It included 69 events in two months
136 of 2014 and 403 events in 2015 that were reported by *Lyu et al.* (2016), and also
137 includes 450 events in 2016 and 412 events in 2017. Fermi operates as a nearly circular
138 orbit at the altitude of 565 km with an inclination of 25.6° and can effectively detect
139 the gamma-ray emissions within the horizontal range of about 600 km from its nadir
140 (*Briggs et al.*, 2010). With the location of +EIPs reported by NLDN and the position
141 of Fermi footprints, the horizontal distances between +EIPs and Fermi nadirs can be
142 obtained. Figure 1a shows the distribution of the horizontal distance between the +EIP
143 location (from NLDN) and the corresponding Fermi nadir point, and Figure 1b shows

144 the geographic distribution of the +EIPs.

145 As illustrated in Figure 1a, a total of 10 +EIPs were found to be located within
 146 600 km away from the Fermi nadir at the +EIP time. The source time of each +EIP
 147 was obtained by subtracting the propagation time between the LF sensor and the +EIP
 148 source, which was supposed at the NLDN horizontal location and an altitude of 12 km
 149 (Cummer *et al.*, 2014; Lyu *et al.*, 2015; Lyu *et al.*, 2018; Pu *et al.*, 2019). Then an
 150 independent search of the gamma-ray photon times recorded by Fermi-GBM time-
 151 tagged events (TTE) data mode and detected by two bismuth germanate (BGO)
 152 scintillation detectors at the source time of each +EIP was conducted. For one of these
 153 +EIPs, the BGO count data are unavailable and this event is excluded from further
 154 analysis. For the remaining 9 +EIPs, the binned histograms of gamma-ray count times
 155 relative to the +EIP time are shown in Figure 1(c).



156

157 **Figure 1.** All +EIPs identified during 2014–2017 and gamma-ray photons of 9 +EIPs
 158 that also reported by Fermi as TGFs. (a) The distribution of the horizontal distance

159 between the NLDN location of each +EIP and the nadir of Fermi at +EIP time. Note
160 that all the +EIPs were in the range of 263 km to ~20,000 km, but only those within the
161 range of 5000 km of a Fermi nadir were illustrated in (a). The horizontal short line
162 enclosed the +EIPs located less than 600 km from Fermi. (b) The geolocation of all the
163 1334 +EIPs (marked by the light blue crosses). The colorful crosses and the circles
164 illustrated the location of the 10 +EIPs enclosed by the short line in (a) and the
165 corresponding Fermi nadir positions. The small light blue crosses mark the geolocation
166 of all other +EIPs with larger distances. (c) The source time difference between Fermi
167 BGO photon counts (binned with 200 μ s window) and the peak of the initial LF pulse
168 of each +EIP.

169

170 **3.1 EIP1 to EIP8 previously reported by Fermi-GBM as TGFs**

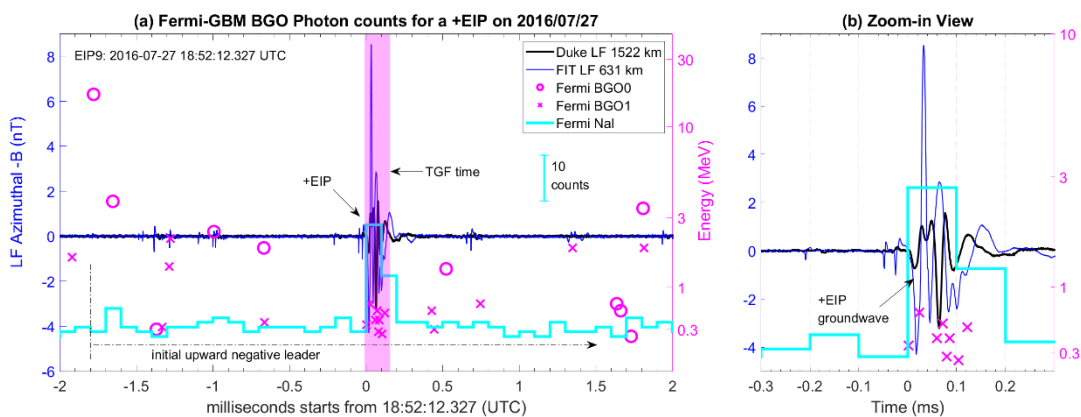
171 The relative distance between the +EIP location and the Fermi nadir can be
172 found in Figure 1(a) by the plots of different colors shown in Figure 1(c). As can be
173 seen in Figure 1(c), EIPs 1–8 were associated with clear bursts of gamma-ray photons
174 within a short time window around the expected time. These 8 TGFs were also
175 identified by the Fermi general TGF identification criteria and reported to be TGFs
176 (*Briggs et al.*, 2013). Three of these 8 are those 3 already analyzed by Lyu et al.
177 (2016) in a preliminary investigation on the relationship between +EIP and TGFs. Thus
178 we show here that during the year 2016-2017, an additional 5 EIP-TGF pairs (EIP4 to
179 EIP8) were found. Even though these 8 TGFs were previously identified, it should be
180 emphasized that here they were found through a search that only used the radio
181 waveforms, radio timing, and source location of the lightning.

182 As shown by the binned histogram plot in Figure 1(c), the peak time of the BGO
 183 gamma-ray count pulses and initial peak times for EIP4-EIP8 are aligned very well in
 184 the 200- μ s bin window. These 8 events further show the very close association between
 185 +EIPs and TGFs in a short time window (usually \sim 200 μ s).

186

187 3.2 EIP9 identifies a new Fermi TGF

188 EIP9 was located at 560 km from its corresponding Fermi nadir, with the
 189 relative distance and locations illustrated by the black plots in Figure 1(a) and 1(b). The
 190 histogram of original gamma-ray photons from both two BGO channels is shown by
 191 the black curve at the bottom of Figure 1(c). A weak pulse of gamma-ray photons
 192 during the short window of EIP9 can be seen, and this event was not reported as a TGF
 193 in the Fermi GBM database. However, a detailed investigation into the Fermi-GBM
 194 gamma-ray photon data indicates that EIP9 is in fact a weak TGF.



195

196 **Figure 2.** The radio signals (blue and black curves) of the EIP-producing leader and
 197 the Fermi-GBM detected BGO photon counts (magenta circles and crosses) and the NaI
 198 histogram (cyan stair plot) during the occurrence of EIP9 on Jul 27, 2016, at
 199 18:52:12.327 (UTC).

200

201 Figure 2 shows the time association of the LF radio signal of EIP9 from two LF
202 sensors (Duke and FIT) and the Fermi-GBM detected gamma-ray photons. Both times
203 were shifted back to the source location of EIP9 by subtracting the speed-of-light
204 propagation delays. The clear LF pulses both before and after EIP9 suggests that it was
205 likely produced during an initial upward IC negative polarity leader approximately 1.8
206 ms after the leader initiation, which is a typical occurrence context of +EIPs (*Lyu et al.*,
207 2015). The magenta crosses and circles indicated the times of gamma-ray photons
208 detected by two BGO detectors (BGO0 and BGO1), respectively. Note that there were
209 no photons detected by BGO0 during the 1 ms window around EIP9, and BGO0
210 recorded only random background counts. Nevertheless, a burst of 8 BGO photons
211 with energy of hundreds of keV from BGO1 and a histogram peak of 24 photons from
212 sodium iodide (NaI) scintillation detectors (energy range of 8 keV to 1 MeV) (*Briggs*
213 *et al.*, 2013) was aligned very well with EIP9 in a ~ 100 μ s window. This strongly
214 indicates that there was a TGF associated with EIP9. The magenta shadow in Figure
215 2(a) indicates the window when the TGF was produced, which is well consistent with
216 the circumstance of EIP1–EIP8 shown in Figure 1(c).

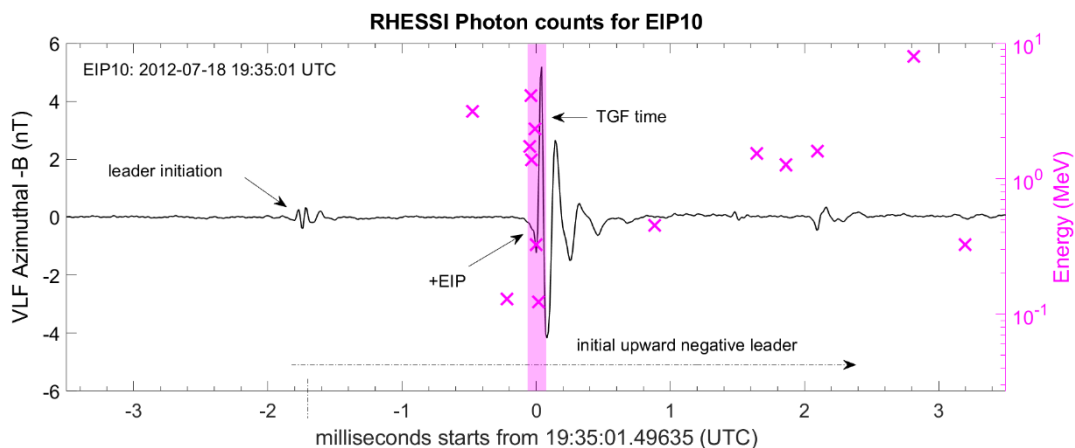
217 TGFs are identified from the Fermi-GBM database using offline analysis of the
218 TTE photon data (*Briggs et al.*, 2013). To reduce the number of false identification due
219 to statistical fluctuations and to ensure sufficient signal to be able to reject cosmic rays
220 effectively, the off-line search requires at least four counts in each BGO detector within
221 a variable time window (*Briggs et al.*, 2013). However, this detection criterion
222 introduces a dependence on the relative position between the spacecraft coordinates and
223 the TGF source. Under certain viewing geometries, only one of the BGO detectors is
224 expected to receive gamma-ray counts from a TGF due to shadowing by the spacecraft.

225 This limits the detection efficiency of some TGFs due to an unfavorable arrival
226 direction in the spacecraft frame (*Roberts et al.*, 2018). And the low energy range of
227 the BGO photons associated with EIP9 (ranging from 140 to 660 keV) is well consistent
228 with the large offset from the Fermi nadir (560 km for EIP9) and that Fermi is outside
229 of the main beam and observing Compton scattered photons, which dynamically
230 decreases the energy of photons (*Østgaard et al.*, 2008; *Celestin & Pasko*, 2012; *Briggs*
231 *et al.*, 2013; *Xu et al.*, 2019). This appears to be the reason that the TGF associated with
232 EIP9 was not identified in the Fermi analysis. However, the data indicate that this is
233 indeed a new TGF, and it was found through this search based on the ground-based
234 measurement of radio signal and timing analysis.

235

236 **4. A new RHESSI TGF identified by ground measurement of +EIPs**

237 The gamma-ray counts detected by RHESSI were also examined to identify any
238 TGF signatures of +EIPs. RHESSI was a NASA Small Explorer spacecraft designed
239 to study x-rays and gamma rays from solar flares, with an orbit of inclination 38° and
240 of altitude 600 km (*Smith et al.*, 2005). It covered most of Earth's thunderstorm zones
241 and detected TGFs with geomagnetic latitudes up to ~50° and detected TGFs effectively
242 for those occurred within 500 km horizontal range of the nadir point. Accounting for
243 the availability of both the radio and photon data, +EIPs in the year 2012 were
244 investigated. Although we archived only limited LF data during 2012, +EIPs were
245 successfully identified from the VLF/ULF radio signals, which also showed
246 distinguishable signatures of the EIP process. The search process was basically the
247 same as that described by Lyu et al. (*Lyu et al.*, 2015).



248

249 **Figure 3.** (a) The VLF radio waveform of the EIP-producing leader and the RHESSI
 250 detected photons during the occurrence of EIP10 on Jul 18, 2012, at 19:35:01 UTC.
 251 The burst of the photons and their energy were marked by the magenta crosses, with
 252 the magenta bar illustrates the time of a TGF.

253

254 For this portion of the analysis, we only focused on the NLDN-identified IC
 255 events with peak current above 100 kA and those located within 1000 km of the
 256 RHESSI footprint. During the calendar year of 2012, a total of 72 NLDN-reported high
 257 peak-current IC events fell into our initial data set. Then with careful investigation and
 258 event discrimination, a total of 13 +EIP events were identified from the archived VLF
 259 and ULF data. There is only one of these +EIPs (EIP10, hereinafter) that was located
 260 within 500 km (315 km) from the RHESSI nadir, which is the effective detection range
 261 of RHESSI. No TGF was reported in the RHESSI TGF catalog during the time window
 262 around EIP10.

263 However, the RHESSI gamma-ray photon data during a short window centered
 264 at the source time of EIP10 reveal that there was a TGF at this time. The radio signals
 265 measured by the Duke VLF sensor and photons detected by the RHESSI gamma-ray

266 detector during a 7-ms window were shown in Figure 3, with the times of both the radio
267 signals and photons were shifted back to the source position of EIP10, which was
268 assumed to be at 12 km above its NLDN ground location. EIP10 was reported by
269 NLDN with a peak current of 195 kA. From the VLF signals recorded at 1279 km, a
270 weak initiation pulse was identified at ~1.9 ms preceding EIP10. The radio pulses both
271 before and after the main EIP pulse suggests an active lightning leader process during
272 the EIP occurrence (*Lyu et al., 2015*). It is remarkable to note that a burst of six photons
273 with energy ranging from ~100 keV to 4.1 MeV were lined up in a 60- μ s window of
274 the initial VLF peak of EIP10. This agrees well with the scenario of EIP-associated
275 Fermi TGFs shown in Figure 1(c) and Figure 2. Comparing to the random photons both
276 before and after EIP10, the burst of high energy photons in such a short window
277 strongly indicates a TGF associated with EIP10. This radio-based search process has
278 thus identified 2 new TGFs, adding to the evidence that most and perhaps all +EIPs are
279 also TGFs.

280

281 **5. Analysis and Significance of EIP-TGF Relationship**

282 Our search for +EIPs from radio and NLDN data required that either Fermi or
283 RHESSI was sufficiently close to the source to detect any possible TGF but was
284 otherwise unbiased from the perspective of TGFs. Of the 10 +EIPs that were
285 sufficiently close to the satellites and for which gamma-ray count data are available, we
286 have found that all 10 are associated with clear and unambiguous TGFs. It should be
287 emphasized that while a +EIP implies a TGF with high certainty, this does not mean
288 that a TGF implies a +EIP with equal certainty. Approximately 90% of TGFs are not
289 associated with +EIPs but are instead associated with less energetic discharge
290 signatures (*Lu et al., 2011; Cummer et al., 2014*), such as the recently identified “slow

291 pulse” TGFs (*Cummer et al.*, 2011; *Pu et al.*, 2019) and those TGFs associated with
292 unclear or weak discharge processes (*Dwyer & Uman*, 2014; *Mailyan et al.*, 2018; *Lu*
293 *et al.*, 2019).

294 We can assess the statistical meaning of this 10-for-10 result using the approach
295 used previously by *Lyu et al.* (*Lyu et al.*, 2016) and compute the likelihood of a 10-for-
296 10 result assuming that +EIPs produce TGFs with a fixed probability p . We use a
297 binomial distribution to identify the range of probabilities that would produce a 10-for-
298 10 observation with greater than 5% likelihood. Any p for which the 10-for-10
299 likelihood is below 5% is unlikely to produce this measurement and thus interpreted as
300 inconsistent with the observation. A straightforward calculation shows that $p = 0.74$
301 yields a 5% probability (0.74^{10}) of generating the 10-for-10 observation. We thus
302 conclude that the observations are consistent with the probability p of a +EIP also being
303 a TGF ranging from 74% to 100%. The observations presented in this study thus
304 indicate that at least most (74%) and perhaps all (100%) +EIPs are also TGFs.

305 This establishes an even stronger link between TGFs and the +EIP-generating
306 process than previous work (*Lyu et al.*, 2016), which has several important
307 consequences. Observations and measurements of +EIPs (for example, using a three-
308 dimensional lightning mapping array or radio broadband interferometer) are also
309 extremely likely to contain key information about the electron acceleration process in
310 TGFs, even in the absence of direct gamma-ray measurements. Detailed measurements
311 of +EIPs alone, such as that recently reported by *Tilles et al.* (*Tilles et al.*, 2020), should
312 thus provide valuable insight into both TGFs and highly energetic lightning leaders.

313 This +EIP-TGF link also enables the detection of TGFs that are not statistically
314 discernable in satellite gamma-ray measurements alone. The two new TGF detections
315 shown here are both relatively weak TGFs that failed key statistical tests for the gamma-

316 ray measurements alone. But the additional precise timing information provided by the
317 simultaneous +EIPs pointed to very short, sub-millisecond time windows to search for
318 gamma-ray pulses, and indeed in these windows, TGFs were found.

319 Lastly, the identification of two new TGFs from ground-based +EIP radio detection
320 not only illustrates the tight connection between +EIPs and TGFs, but also further
321 demonstrated the practicability of detecting a subset of TGFs from ground radio
322 measurements alone. Ground-based detection of TGFs from long-distance radio
323 measurements can strongly complement space-based detection of TGFs.

324

325 **6. Discussion and Conclusions**

326 Energetic in-cloud pulses, or EIPs, are a recently identified class of high peak-
327 current lightning events that occur sometimes during the progression of lightning in-
328 cloud negative leaders (*Lyu et al.*, 2015; *Lyu & Cummer*, 2018). They can be robustly
329 detected and reliably identified using signals from distant ground-based radio sensors.
330 In this study, an expanded radio-only search for positive polarity energetic in-cloud
331 pulses (+EIPs) yielded 10 events that occurred within the TGF-detection range of the
332 Fermi and RHESSI spacecrafts at times when gamma-ray photon data exist. The
333 simultaneous gamma-ray photon data show that all 10 +EIPs are also TGFs, including
334 two TGFs not previously identified by the routine TGF identification criteria of two
335 different space-based detectors. The 10 out of 10 EIP-TGF pairs are consistent with a
336 range of 74% to 100% for the probability that a given +EIP is also a TGF. Remarkably,
337 the identification of two previously unreported new TGFs from the detection of +EIPs
338 further validated their close relationship.

339 Collectively, the results shown in this study presented strong evidence that most
340 and perhaps all +EIPs are TGFs. We emphasize that the converse is not true because
341 only about 10% of all TGFs are associated with high peak current +EIPs. The definitive
342 EIP-TGF connection also implies a link between the processes involved in TGF
343 production and the processes that produce strong, transient, >100 kA equivalent peak
344 current pulses during the propagation of upward negative leaders. A recent study on
345 EIPs using very high frequency (VHF) broadband interferometry and electromagnetic
346 field measurements (*Tilles et al., 2020*) conducted a detailed analysis on the radio
347 emission of the +EIP source. Those results, plus our new findings here, continue to
348 suggest that the +EIP spheric is, to a large extent, not produced by normal lightning leader
349 processes. This is similar to what has been found previously for a distinct class of TGFs,
350 the so-called “isolated slow pulse” TGFs (*Cummer et al., 2011; Pu et al., 2019*). The
351 +EIP and the “slow pulse” processes do share several common features between them,
352 including the close temporal association with TGFs, the occurrence the pulse during
353 upward negative initial leaders, and the time scale of the pulse (~50-100 μ s). However,
354 the peak radiated field of +EIPs is typically more than an order of larger than that of
355 the slow pulses, and the waveform of a typical +EIP is much more complex than a slow
356 pulse. Both +EIPs and the slow pulses appear to be produced at least partly by the
357 relativistic electron acceleration in the TGF production (*Dwyer, 2012; Liu & Dwyer,*
358 *2013*) and not by standard lightning processes.

359 An important element of this research is the identification of two previously
360 unreported new TGFs from the detection of +EIPs. This finding not only adds key
361 support to the EIP-TGF connection, but also, for the first time, experimentally
362 demonstrates the idea of detecting a subset of TGFs from ground-based radio
363 measurements alone (*Lyu et al., 2016*). The ability to detect a subset of TGFs through

364 ground-based, radio-only measurements will significantly improve obtaining more
365 detailed measurements of the lightning processes responsible for producing TGFs. This
366 type of TGF detection can be a valuable addition to satellite gamma-ray detector-based
367 detection, especially during time windows or in locations where space-based detectors
368 are not available.

369 These results also strengthen the connection between TGFs and transient
370 luminous events, specifically in the form of elves (*Lyu et al., 2015*), seen as optical
371 emissions at the altitude of lower ionosphere because of the transient field change from
372 energetic electromagnetic field pulses. Modeling suggested that elves may accompany
373 with TGFs associated with EIPs (*Liu et al., 2017*). This connection was confirmed by
374 a recent study reporting a simultaneous observation of a TGF and elve (*Neubert et al.,*
375 *2020*) associated with a radio pulse that seems likely to also have been a +EIP. The
376 detection of +EIPs from the ground is thus a useful method to perform observations and
377 detailed studies of the connection between different energetic atmospheric electricity
378 processes including EIPs, TGFs, and elves during thunderstorms.

379

380 **Acknowledgment**

381 The authors would like to acknowledge support from the National Science
382 Foundation Dynamic and Physical Meteorology program (grant AGS-2026304), the
383 Open Grants of the State Key Laboratory of Severe Weather of China (grant
384 2020LASW-A02), the National Science Foundation (grant ATM-0846609 and grant
385 ATM-1935989), and the National Aeronautics and Space Administration (grant
386 NNM11AA01A). This work complies with the AGU data policy. The radio waveforms,
387 NLDN reported information, the RHESSI and Fermi-GBM photon counts are available

388 at XX (the link will be provided later). The Fermi BGO photon counts are also available
389 at <https://heasarc.gsfc.nasa.gov/FTP/fermi/data/gbm/daily/>.

390

391 **Reference**

392 Briggs, M. S., Fishman, G. J., Connaughton, V., Bhat, P. N., Paciesas, W. S., Preece,
393 R. D., Wilson-Hodge, C., Chaplin, V. L., Kippen, R. M., von Kienlin, A., et al.
394 (2010). First results on terrestrial gamma ray flashes from the Fermi Gamma-
395 ray Burst Monitor. *Journal of Geophysical Research: Space Physics*, *115*(A7),
396 doi:10.1029/2009JA015242.

397 Briggs, M. S., Xiong, S. L., Connaughton, V., Tierney, D., Fitzpatrick, G., Foley, S.,
398 Grove, J. E., Chekhtman, A., Gibby, M., Fishman, G. J., et al. (2013). Terrestrial
399 gamma-ray flashes in the Fermi era: Improved observations and analysis
400 methods. *Journal of Geophysical Research-Space Physics*, *118*(6), 3805-3830,
401 doi:10.1002/jgra.50205.

402 Celestin, S., & Pasko, V. P. (2012). Compton scattering effects on the duration of
403 terrestrial gamma-ray flashes. *Geophysical Research Letters*, *39*,
404 doi:10.1029/2011GL050342.

405 Connaughton, V., Briggs, M. S., Holzworth, R. H., Hutchins, M. L., Fishman, G. J.,
406 Wilson-Hodge, C. A., Chaplin, V. L., Bhat, P. N., Greiner, J., von Kienlin, A.,
407 et al. (2010). Associations between Fermi Gamma-ray Burst Monitor terrestrial
408 gamma ray flashes and sferics from the World Wide Lightning Location
409 Network. *Journal of Geophysical Research-Space Physics*, *115*,
410 doi:10.1029/2010JA015681.

411 Cummer, S. A., Lu, G. P., Briggs, M. S., Connaughton, V., Xiong, S. L., Fishman, G.
412 J., & Dwyer, J. R. (2011). The lightning-TGF relationship on microsecond
413 timescales. *Geophysical Research Letters*, *38*, doi:10.1029/2011GL048099.

414 Cummer, S. A., Briggs, M. S., Dwyer, J. R., Xiong, S. L., Connaughton, V., Fishman,
415 G. J., Lu, G. P., Lyu, F. C., & Solanki, R. (2014). The source altitude, electric
416 current, and intrinsic brightness of terrestrial gamma ray flashes. *Geophysical*
417 *Research Letters*, *41*(23), 8586-8593

418 Dwyer, J. R. (2012). The relativistic feedback discharge model of terrestrial gamma ray

- 419 flashes. *JOURNAL OF GEOPHYSICAL RESEARCH*, 117(A2),
420 doi:10.1029/2011JA017160.
- 421 Dwyer, J. R., Smith, D. M., & Cummer, S. A. (2012). High-Energy Atmospheric
422 Physics: Terrestrial Gamma-Ray Flashes and Related Phenomena. *Space*
423 *Science Reviews*, 173(1), 133-196, doi:10.1007/s11214-012-9894-0.
- 424 Dwyer, J. R., & Cummer, S. A. (2013). Radio emissions from terrestrial gamma-ray
425 flashes. *Journal of Geophysical Research-Space Physics*, 118(6), 3769-3790,
426 doi:10.1002/jgra.50188.
- 427 Dwyer, J. R., & Uman, M. A. (2014). The physics of lightning. *Physics Reports-Review*
428 *Section of Physics Letters*, 534(4), 147-241, doi:10.1016/j.physrep.2013.09.004.
- 429 Dwyer, J. R., Liu, N. Y., Grove, J. E., Rassoul, H., & Smith, D. M. (2017).
430 Characterizing the source properties of terrestrial gamma ray flashes. *Journal*
431 *of Geophysical Research-Space Physics*, 122(8), 8915-8932,
432 doi:10.1002/2017JA024141.
- 433 Fishman, G. J., Bhat, P. N., Mallozzi, R., Horack, J. M., Koshut, T., Kouveliotou, C.,
434 Pendleton, G. N., Meegan, C. A., Wilson, R. B., Paciasas, W. S., et al. (1994).
435 Discovery of intense gamma-ray flashes of atmospheric origin. *Science*,
436 264(5163), 1313-1316, doi:10.1126/science.264.5163.1313.
- 437 Liu, N., & Dwyer, J. R. (2013). Modeling terrestrial gamma ray flashes produced by
438 relativistic feedback discharges. *Journal of Geophysical Research-Space*
439 *Physics*, 118(5), 2359-2376, doi:10.1002/jgra.50232.
- 440 Liu, N., Dwyer, J. R., & Cummer, S. A. (2017). Elves Accompanying Terrestrial
441 Gamma Ray Flashes. *Journal of Geophysical Research-Space Physics*, 122(10),
442 10563-10576, doi:10.1002/2017JA024344.
- 443 Lu, G., Blakeslee, R. J., Li, J., Smith, D. M., Shao, X.-M., McCaul, E. W., Buechler,
444 D. E., Christian, H. J., Hall, J. M., & Cummer, S. A. (2010). Lightning mapping
445 observation of a terrestrial gamma-ray flash. *Geophysical Research Letters*,
446 37(11), doi:10.1029/2010GL043494.
- 447 Lu, G., Cummer, S. A., Li, J. B., Han, F., Smith, D. M., & Grefenstette, B. W. (2011).
448 Characteristics of broadband lightning emissions associated with terrestrial
449 gamma ray flashes. *Journal of Geophysical Research-Space Physics*, 116,
450 doi:10.1029/2010JA016141.
- 451 Lu, G., Zhang, H. B., Cummer, S. A., Wang, Y. P., Lyu, F. C., Briggs, M., Xiong, S.

- 452 L., & Chen, A. (2019). A comparative study on the lightning sferics associated
453 with terrestrial gamma-ray flashes observed in Americas and Asia. *Journal of*
454 *Atmospheric and Solar-Terrestrial Physics*, 183, 67-75,
455 doi:10.1016/j.jastp.2019.01.001.
- 456 Lyu, F., Cummer, S. A., & McTague, L. (2015). Insights into high peak current in-
457 cloud lightning events during thunderstorms. *Geophysical Research Letters*,
458 42(16), 6836-6843, doi:10.1002/2015GL065047.
- 459 Lyu, F., Cummer, S. A., Briggs, M., Marisaldi, M., Blakeslee, R. J., Bruning, E., Wilson,
460 J. G., Rison, W., Krehbiel, P., Lu, G., et al. (2016). Ground detection of
461 terrestrial gamma ray flashes from distant radio signals. *Geophysical Research*
462 *Letters*, 43(16), 8728-8734, doi:10.1002/2016GL070154.
- 463 Lyu, F., & Cummer, S. A. (2018). Energetic Radio Emissions and Possible Terrestrial
464 Gamma-Ray Flashes Associated With Downward Propagating Negative
465 Leaders. *Geophysical Research Letters*, 45(19), 10764-10771,
466 doi:10.1029/2018GL079424.
- 467 Lyu, F., Cummer, S. A., Krehbiel, P. R., Rison, W., Briggs, M. S., Crame, E., Roberts,
468 O., & Stanbro, M. (2018). Very High Frequency Radio Emissions Associated
469 With the Production of Terrestrial Gamma-Ray Flashes. *Geophysical Research*
470 *Letters*, 45(4), 2097-2105, doi:10.1002/2018GL077102.
- 471 Mailyan, B. G., Nag, A., Murphy, M. J., Briggs, M. S., Dwyer, J. R., Rison, W.,
472 Krehbiel, P. R., Boggs, L., Bozarth, A., Cramer, E. S., et al. (2018).
473 Characteristics of Radio Emissions Associated With Terrestrial Gamma-Ray
474 Flashes. *Journal of Geophysical Research-Space Physics*, 123(7), 5933-5948,
475 doi:10.1029/2018JA025450.
- 476 Marisaldi, M., Fuschino, F., Labanti, C., Galli, M., Longo, F., Del Monte, E., Barbiellini,
477 G., Tavani, M., Giuliani, A., Moretti, E., et al. (2010). Detection of terrestrial
478 gamma ray flashes up to 40 MeV by the AGILE satellite. *Journal of*
479 *Geophysical Research: Atmospheres*, 115(A3), doi:10.1029/2009JA014502.
- 480 Neubert, T., Ostgaard, N., Reglero, V., Blanc, E., Chanrion, O., Oxborrow, C. A., Orr,
481 A., Tacconi, M., Hartnack, O., & Bhandari, D. D. V. (2019). The ASIM Mission
482 on the International Space Station. *Space Science Reviews*, 215(2),
483 doi:10.1007/s11214-019-0592-z.
- 484 Neubert, T., Ostgaard, N., Reglero, V., Chanrion, O., Heumesser, M., Dimitriadou, K.,

- 485 Christiansen, F., Budtz-Jorgensen, C., Kuvvetli, I., Rasmussen, I. L., et al.
486 (2020). A terrestrial gamma-ray flash and ionospheric ultraviolet emissions
487 powered by lightning. *Science*, 367(6474), 183-186,
488 doi:10.1126/science.aax3872.
- 489 Østgaard, N., Gjesteland, T., Stadsnes, J., Connell, P. H., & Carlson, B. (2008).
490 Production altitude and time delays of the terrestrial gamma flashes: Revisiting
491 the Burst and Transient Source Experiment spectra. *Journal of Geophysical*
492 *Research-Atmospheres*, 113(A2), doi:10.1029/2007ja012618.
- 493 Østgaard, N., Gjesteland, T., Carlson, B. E., Collier, A. B., Cummer, S. A., Lu, G., &
494 Christian, H. J. (2013). Simultaneous observations of optical lightning and
495 terrestrial gamma ray flash from space. *Geophysical Research Letters*, 40(10),
496 2423-2426, doi:10.1002/grl.50466.
- 497 Pu, Y., Cummer, S. A., Lyu, F., Briggs, M., Mailyan, B., Stanbro, M., & Roberts, O.
498 (2019). Low Frequency Radio Pulses Produced by Terrestrial Gamma-Ray
499 Flashes. *Geophysical Research Letters*, 46(12), 6990-6997,
500 doi:10.1029/2019GL082743.
- 501 Roberts, O. J., Fitzpatrick, G., Stanbro, M., McBreen, S., Briggs, M. S., Holzworth, R.
502 H., Grove, J. E., Chekhtman, A., Cramer, E. S., & Mailyan, B. G. (2018). The
503 First Fermi-GBM Terrestrial Gamma Ray Flash Catalog. *Journal of*
504 *Geophysical Research-Space Physics*, 123(5), 4381-4401,
505 doi:10.1029/2017JA024837.
- 506 Shao, X. M., Hamlin, T., & Smith, D. M. (2010). A closer examination of terrestrial
507 gamma-ray flash-related lightning processes. *Journal of Geophysical Research-*
508 *Space Physics*, 115(A00E30), doi:10.1029/2009JA014835.
- 509 Smith, D. M., L. I. Lopez, R. P. Lin, & Barrington-Leigh, C. P. (2005). Terrestrial
510 gamma-ray flashes observed up to 20 MeV. *Science*, 307(5712), 1085-1088,
511 doi:10.1126/science.1107466.
- 512 Stanley, M. A., Shao, X. M., Smith, D. M., Lopez, L. I., Pongratz, M. B., Harlin, J. D.,
513 Stock, M., & Regan, A. (2006). A link between terrestrial gamma-ray flashes
514 and intracloud lightning discharges. *Geophysical Research Letters*, 33(6),
515 doi:10.1029/2005GL025537.
- 516 Tilles, J. N., Krehbiel, P. R., Stanley, M. A., Rison, W., Liu, N., Lyu, F., Cummer, S.
517 A., Dwyer, J. R., Senay, S., Edens, H., et al. (2020). Radio Interferometer

518 Observations of an Energetic in-Cloud Pulse Reveal Large Currents Generated
519 by Relativistic Discharges. *Journal of Geophysical Research-Atmospheres*,
520 125(20), e2020JD032603, doi:10.1029/2020jd032603.

521 Xu, W., Celestin, S., Pasko, V. P., & Marshall, R. A. (2019). Compton Scattering
522 Effects on the Spectral and Temporal Properties of Terrestrial Gamma-Ray
523 Flashes. *Journal of Geophysical Research-Space Physics*, 124(8), 7220-7230,
524 doi:10. 1029/2019JA026941.

525 Zhang, H., Lu, G., Lyu, F., Ahmad, M. R., Qie, X., Cummer, S. A., Xiong, S., & Briggs,
526 M. S. (2020). First Measurements of Low-Frequency Sferics Associated With
527 Terrestrial Gamma-Ray Flashes Produced by Equatorial Thunderstorms.
528 *Geophysical Research Letters*, 47(17), e2020GL089005,
529 doi:10.1029/2020gl089005.

530